AJNR

Evaluation of Treatment-Induced Cerebral White Matter Injury by Using Diffusion-Tensor MR Imaging: Initial Experience

Sawako Kitahara, Satoshi Nakasu, Kiyoshi Murata, Keizen Sho and Ryuta Ito

AJNR Am J Neuroradiol 2005, 26 (9) 2200-2206
http://www.ajnr.org/content/26/9/2200

Evaluation of Treatment-Induced Cerebral White Matter Injury by Using Diffusion-Tensor MR Imaging: Initial Experience

Sawako Kitahara, Satoshi Nakasu, Kiyoshi Murata, Keizen Sho, and Ryuta Ito

BACKGROUND AND PURPOSE: **Treatment with chemotherapy and radiation therapy for brain tumors can cause white matter (WM) injury. Conventional MR imaging, however, cannot always depict treatment-induced transient WM abnormalities. We investigated the ability of diffusion-tensor (DT) MR imaging and proton MR spectroscopy to detect the treatment-induced transient changes within normal-appearing WM.**

METHODS: **DT MR imaging and proton MR spectroscopy were performed in 8 patients treated with a combination of surgery, chemotherapy, and radiation therapy for brain tumors (17 examinations) and 11 age-matched controls. Apparent diffusion coefficient (ADC) value, fractional anisotropy (FA) value, and *N*-acetylaspartate (NAA)/creatine (Cr) ratio were obtained from 27 hemispheres with normal-appearing WM in the patients. We divided the datasets of isotropic ADC, FA, and NAA/Cr, on the basis of the time period after completion of radiation therapy, into 4 groups: group 1 (0–2 months; $n = 10$), group 2 (3–5 months; $n = 5$), group 3 (6–9 months; $n = 7$), and group 4 (10–12 months; $n = 5$). We compared averages of mean isotropic ADC, mean FA, and NAA/Cr of each patient group with those of the control group by using a *t* test.**

RESULTS: **In the group 2, averages of mean FA and NAA/Cr decreased and average of mean isotopic ADC increased in comparison with those of the control group ($P = .004$, .04, and .0085, respectively). There were no significant differences in the averages between the control group and patient groups 1, 3, and 4.**

CONCLUSION: **DT MR imaging and proton MR spectroscopy can provide quantitative indices that may reflect treatment-induced transient derangement of normal-appearing WM.**

The combination of surgery, chemotherapy, and radiation therapy plays an important role in the treatment of primary and metastatic brain tumors. External beam radiation and chemotherapy, however, cause various pathologic side effects that include transient and/or long-term injuries to the normal brain tissue (1–3). Although treatment-induced transient white matter (WM) changes on the conventional MR images have been reported (2–5), they cannot always describe visible abnormalities in the patients with symptoms. Objective, sensitive, and quantitative methods to evaluate treatment-induced transient injuries are required because monitoring of treatment-induced neurotoxicity is important for determining appropriate schedule of additional therapy and minimizing adverse effects to the normal brain tissues. Diffusion-tensor (DT) MR imaging (6) and proton MR spectroscopy allow quantitative investigation of the changes in the metabolite levels and water diffusion parameters within visually normal-appearing WM on the conventional MR images. In children treated with combination therapy for medulloblastoma, DT MR imaging has revealed long-term reduction of anisotropy in normal-appearing WM (7). Proton MR spectroscopy study has shown transient reduction of *N*-acetylaspartate (NAA)/creatine (Cr) ratios in the normal brain parenchyma in the subacute phase after radiation therapy (8). To the best of our knowledge, no report has attempted to evaluate treatment-induced transient changes in normal-appearing WM by using DT MR imaging. Thus, the purpose of this study is to assess whether isotropic apparent diffusion coefficient (ADC) and fractional anisotropy (FA) values derived from DT MR imaging (9) and NAA/Cr ratio obtained by single-voxel proton MR spectroscopy can be used as quantitative indices

Received December 21, 2004; accepted after revision March 1, 2005.

Presented at the 41st annual meeting of American Society of Neuroradiology, Washington, D.C., April 26–May 2, 2003.

From the Departments of Radiology (S.K., K.M., K.S., R.I.) and Neurosurgery (S.N.), Shiga University of Medical Science, Shiga, Japan.

Address correspondence to Sawako Kitahara, MD, Department of Radiology, Shiga University of Medical Science, Seta Tsukinowa-cho, Otsu, Shiga 520-2192, Japan.

TABLE 1: Clinical characteristics and therapeutic regimens

Patient No./ Age (y)/Sex	Brain Tumor	Surgery	Radiotherapy (dose/Fx)	Chemotherapy
1/70/M	Malignant lymphoma	Biopsy	40 Gy WB with 14 Gy boost/22 Fx	MTX
2/53/F	Malignant lymphoma	None	40 Gy WB with 14 Gy boost/28 Fx	MTX, ICE
3/55/F	Metastatic tumor (pulmonary adenocarcinoma)	Total removal	30 Gy WB/10 Fx	None
4/53/M	Glioblastoma	Partial removal	30 Gy WB/15 Fx	CE, other
5/64/M	Metastatic tumor (pulmonary adenocarcinoma)	Total removal	30 Gy WB with 15 Gy boost (stereotactic radiosurgery)/11 Fx	None
6/61/F	Malignant lymphoma	Biopsy	30 Gy WB/14 Fx	MTX, ICE, other*
7/21/M	Medulloblastoma	Partial removal	32 Gy WB with 22 Gy boost/22 Fx	ICE, CE
8/26/M	Pineal germinoma	Biopsy	30 Gy WB with 20 Gy boost/20 Fx	CE

Note.—WB indicates whole brain; Fx, fraction; MTX, methotrexate; ICE, ifosfamide, carboplatin, and etoposide; CE, carboplatin and etoposide; other, other chemotherapy (nimustine, vincristine, procarbazine); other*, intrathecal chemotherapy (rituximab).

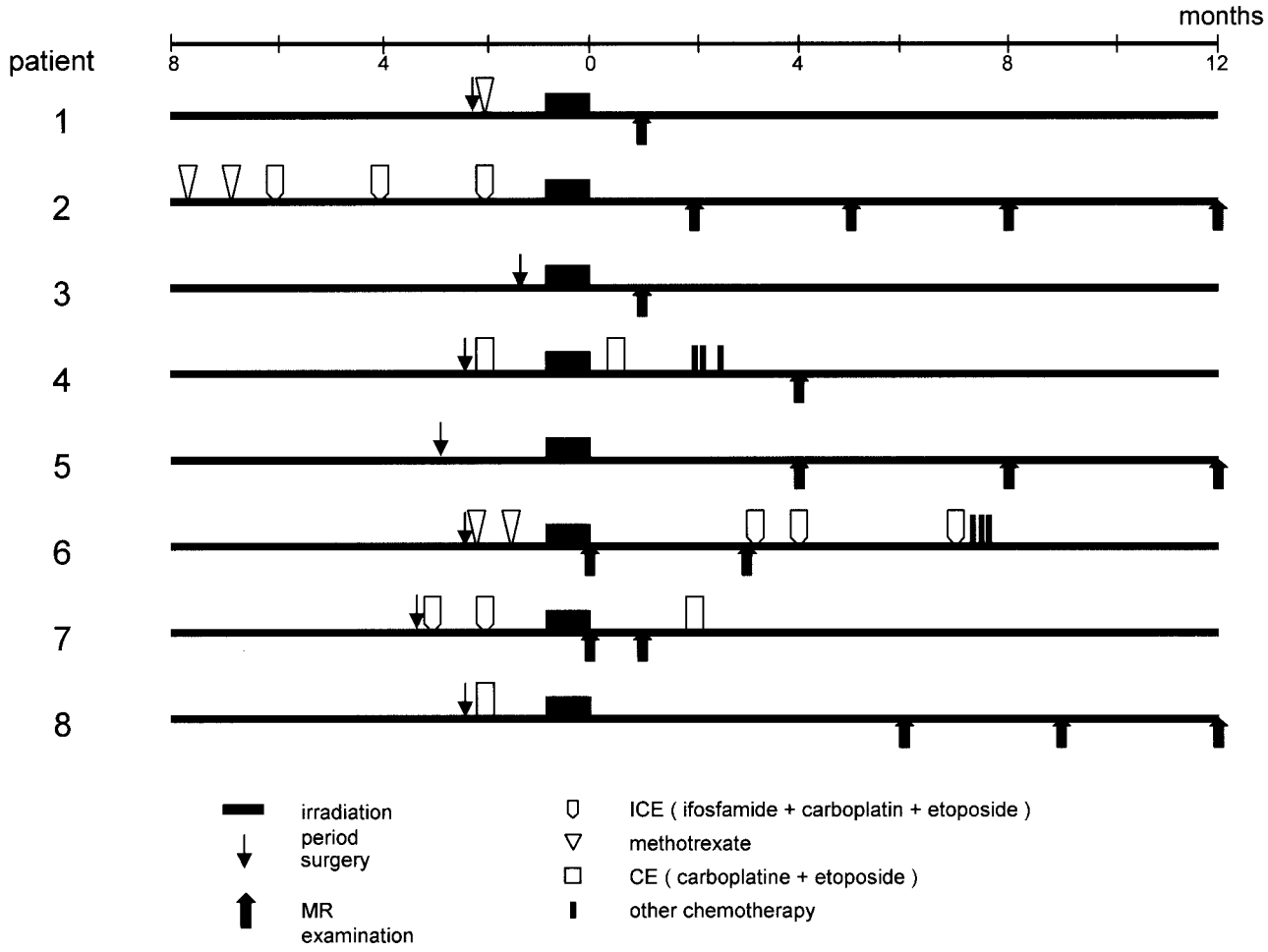

FIG 1. Schedule of surgery, chemotherapy, radiation therapy, and MR examination.

for evaluation of the transient adverse change within normal-appearing WM in patients treated for brain tumors.

Methods

Patients and Controls

Ten patients presented to the department of neurosurgery in our institution with brain tumors and received radiation therapy from November 2001 to July 2002. Two patients, one with difficulty in undergoing MR examination because of disease progression and the other with multiple tumors in both hemispheres, were excluded. The remaining 8 patients (5 men and 3 women; age range, 26–70 years, one glioblastoma, one medulloblastoma, one germinoma, 3 malignant lymphomas, and 2 metastatic brain tumors) were enrolled in this study. The detailed clinical characteristics, schedule of MR examination, and therapeutic regimens employed for these patients are shown in Table 1 and Fig 1. Four patients underwent tumor resection

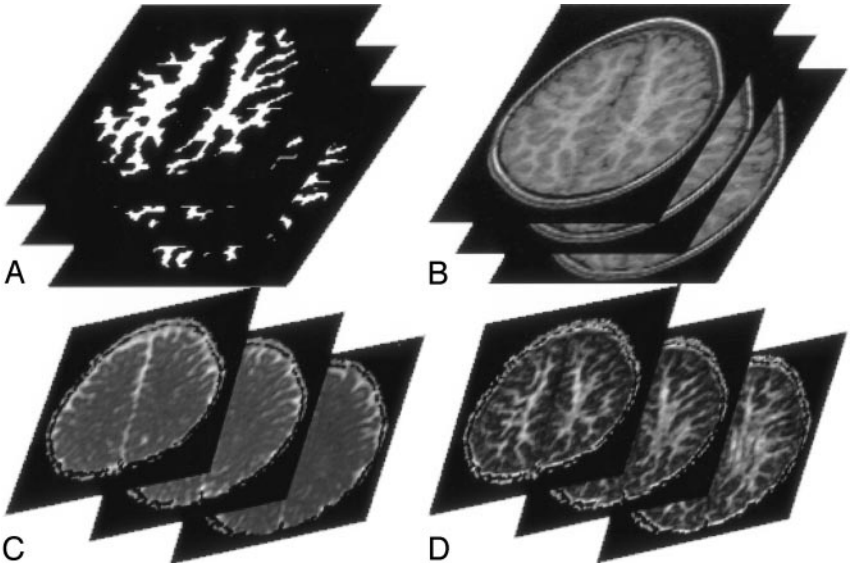

FIG 2. A 42-year-old male control subject. Three continuous section locations in the supraventricular plane.

A, WM segmented automatically from the reprocessed 3D SPGR T1-weighted images (1.9/9.2/1 [TE/TR/NEX]).

B, Reprocessed axial 3D SPGR images.

C, Isotropic ADC maps.

D, FA maps. Means of isotropic ADC and FA values of the pixels within the segmented WM of each hemisphere are calculated.

and 3 underwent biopsy examination within 4 months before completion of radiation therapy. For all patients, at least 30 Gy of irradiation was administered to the whole cranium. In total, they received 30–60 Gy with or without a local boost to the tumor in 10–28 fractions during the course of 11–52 days. Six patients received chemotherapy treatment within 8 months before completion of radiation therapy, and 3 of them received additional chemotherapy after the radiation therapy. Five of these patients received systemic chemotherapy, and one received systemic and intrathecal chemotherapy.

Eleven age-matched controls (7 men and 4 women; age range, 26–72 years) participated in this study. These subjects were healthy volunteers who had neither symptoms nor abnormal neurologic signs.

We obtained an informed consent from all participants before MR scanning. The institutional ethical committee approved this study.

MR Data Acquisition and Analysis

Conventional MR imaging, DT MR imaging, and single-voxel proton MR spectroscopy were performed by using a 1.5T clinical MR system with a standard quadrature head coil.

For DT MR imaging, diffusion-weighted images and images without diffusion sensitization (*b*0 images) of 20 axial locations with 5-mm thickness and 1.5-mm gap were obtained by using a single-shot spin-echo echo-planar readout with peripheral gating (TR/TE, 4918–5625 ms/94 ms; field of view, 22 cm; scan matrix, 96 × 96). Diffusion-sensitizing gradients were applied in 6 different directions, with *b* value of 1000 s/mm^2. We generated pixel-by-pixel maps of isotropic ADC and FA values from the diffusion-weighted images and *b*0 images by using software developed by IDL (Interactive Data Language; Research Systems, Boulder, CO). 3D spoiled gradient (3D SPGR) echo T1-weighted images (TR/TE, 9.2 ms/1.9 ms; field of view, 22 cm; scan matrix, 256 × 128; 1 mm thick) were obtained for tissue segmentation. We reprocessed the T1-weighted images that had the same imaging thickness and locations as the *b*0 images and then segmented WM from the T1-weighted images automatically by using brain image analysis tool, FSL (FMRIB Image Analysis Group, Oxford, UK [10–12]; Fig 2*A*). A transverse supraventricular plane that included 3 continuous section locations starting inferiorly from the top of the lateral ventricles, where the corpus callosum did not exist, was determined (Fig 2*B*). We extracted pixels within the segmented WM in the supraventricular plane and obtained isotropic ADC and FA values of the pixels from corresponding isotropic ADC and FA maps (Fig 2*C, -D*). The mean isotropic ADC and FA values of the extracted pixels within WM of each cerebral hemisphere were calculated. These steps were automatically processed by using the image analysis software, except for determination of the initial section above lateral ventricles. The procedures were identically applied to both patient data and control data.

Proton MR spectra were obtained by using a commercially available point-resolved spectroscopy sequence (TR/, 6000 ms/30 ms). We placed a rectangular volume of interest (VOI) with 18-mm thickness (corresponding to the thickness of the supraventricular plane) within WM of each hemisphere in the same supraventricular plane as DT MR imaging (Fig 3). The VOI size was determined such that the VOI included as much WM as possible (7.6 mL–23.1 mL). We measured the NAA/Cr ratio in the VOI by using LCModel method (13).

For the 8 patients, we performed 17 DT MR imaging and proton MR spectroscopy examinations within 1–372 days (mean, 152.2 days) after completion of radiation therapy. Although therapeutic treatments for the patients in this study were inhomogeneous, all the patients received radiation therapy. Radiation-induced reactions are categorized as acute, subacute, and late delayed effects, and transient effects may occur in the acute phase, within 2 months, and in the subacute phase, 2–6 months after cranial irradiation (1, 14, 15). With reference to MR spectroscopy studies that reported adverse metabolic effects of radiation therapy (8, 16), to evaluate the transient reaction effectively we divided the datasets on the basis of the time period after completion of radiation therapy into 4 groups: group 1, 0–2 months; group 2, 3–5 months; group 3, 6–9 months; group 4, >9 months.

Two radiologists (S.K., R.I.) judged together and determined whether WM in the supraventricular plane appeared normal by means of consensus on the basis of T2-weighted images (fast spin-echo sequence; TR/effective TE/echo train length, 4000 ms/95 ms/18; scan matrix, 320 × 256; the same imaging thickness and locations as the diffusion-weighted images).

Averages of mean isotropic ADC value, mean FA value, and NAA/Cr ratio of each patient group were calculated. Averages of mean isotropic ADC value, mean FA value, and NAA/Cr ratio for normal controls were also calculated. We compared the averages of mean isotropic ADC value, mean FA value, and NAA/Cr ratio of the control group with those of each patient group by using the *t* test. A *P* value $<.05$ was considered to indicate a statistically significant difference.

TABLE 2: Averages of NAA/Cr, mean isotropic ADC value, and mean FA value of control group and four patient groups

Group	NAA/Cr	*P*	Isotropic ADC ($\times 10^{-3}$ mm/2/s)	*P*	FA	*P*
Controls	1.31 ± 0.18		0.692 ± 0.014		0.38 ± 0.02	
1 (0–2 mo)	1.28 ± 0.26	.77	0.696 ± 0.016	.06	0.38 ± 0.02	.91
2 (3–5 mo)	1.13 ± 0.10	.04	0.724 ± 0.060	<.01	0.34 ± 0.04	<.01
3 (6–9 mo)	1.23 ± 0.07	.26	0.687 ± 0.018	.52	0.39 ± 0.03	.57
4 (10–12 mo)	1.28 ± 0.09	.78	0.710 ± 0.007	.12	0.40 ± 0.03	.10

Note.—NAA/Cr indicates *N*-acetylaspartate to creatine ratio; ADC, apparent diffusion coefficient; FA, fractional anisotropy. Values are expressed as mean ± SD. *P* values were obtained by comparison between the values of each patient group versus those of the control group.

Results

For the patients, the datasets of mean isotropic ADC value, mean FA value, and NAA/Cr ratio were successfully acquired from 27 hemispheres that were judged as normal-appearing WM. We divided the 27 datasets into the 4 groups: group 1 ($n = 10$), group 2 ($n = 5$), group 3 ($n = 7$), and group 4 ($n = 5$). For the controls, we successfully obtained NAA/Cr ratios from 18 hemispheres and means of isotropic ADC and FA values from 20 hemispheres. No abnormality was identified in these hemispheres.

The averages of NAA/Cr ratio, mean isotropic ADC value, and FA value of the control group and those of the 4 patient groups are shown in Table 2 and are presented graphically in Fig 4*A–C*. There were no significant differences between the control group and group 1, between the control group and group 3, and between the control group and group 4. In group 2, the averages of NAA/Cr ratio and mean FA value decreased significantly and average of mean isotropic ADC value increased significantly in comparison with those of the control group.

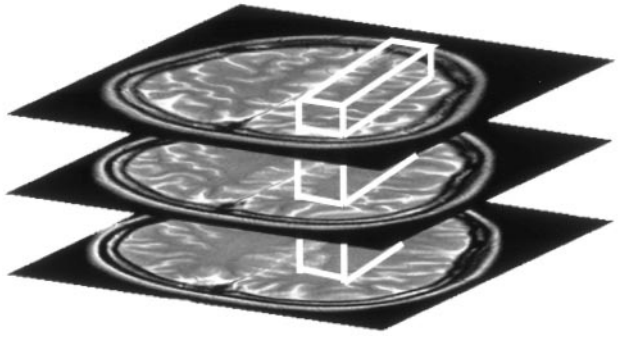

FIG 3. A VOI for proton MR spectroscopy is placed within WM in the same supraventricular plane, from which DT MR imaging indices are derived.

Discussion

After treatments for brain tumors, transient visible changes in WM on conventional MR images have been reported (4). They, however, cannot always describe visible abnormalities in the patients with symptoms (5). On the other hand, neuropsychological tests have not revealed consistent results about the incidence and severity of treatment-related transient neurologic symptoms (14, 15, 17). Distinguishing the relative contributions to the symptoms resulting from the tumor itself, the surgical procedures, radiation therapy, and chemotherapy seems difficult (18). The treatment-induced transient effects are supposed to be secondary to diffuse demyelination histologically (1, 3). There may be "occult" and "invisible" changes in normal-appearing WM. Although the changes are usually reversible, additional treatment while demyelination exists may induce irreversible changes. Moreover, the relationship between the transient changes in normal WM and delayed effects—including cognitive deteriorations—has to be revealed. Objective and quantitative monitoring of normal-appearing WM after the treatment seem to be essential to optimizing the therapeutic regimens and schedule, resulting in minimizing adverse effects to the normal brain tissues. In this study, we showed the potential power of indices derived from DT MR imaging to detect transient changes in normal-appearing WM (Fig 5). A transient decrease in mean FA value and a transient increase in mean isotropic ADC value were observed in the patients as compared with healthy control subjects, and a transient reduction of NAA/Cr ratio in the patients was also revealed by proton MR spectroscopy. By adding ~5 minutes of DT MR imaging to the clinical follow-up MR examination, it is possible to acquire the valuable quantitative indices for the management of the patients treated for brain tumors.

Changes of diffusion properties of the brain with normal-appearing WM on the conventional MR images have been reported in various pathologic conditions such as multiple sclerosis (19, 20), treatment-induced WM injuries in children with medulloblastoma (7), and aging brain (21). These reports suggest that the indices derived from diffusion MR imaging are sensitive to changes in the interstitial space volume and constituents in WM beyond the visible intensity change on the conventional MR images. The observed changes of indices have been considered to represent water content change due to permeability alteration of capillary walls and/or the ordered structural loss including demyelination and axonal fiber loss (22, 23). Radiation therapy and chemotherapy induce transient histopathologic WM changes, which are small vessel injury (alteration of the small vessel wall permeability) and result in edema and consequent demyelination (24, 25). In the present study, these histopathologic changes may contribute to the observed transient changes of indices (ie, decrease in mean FA value and increase in mean

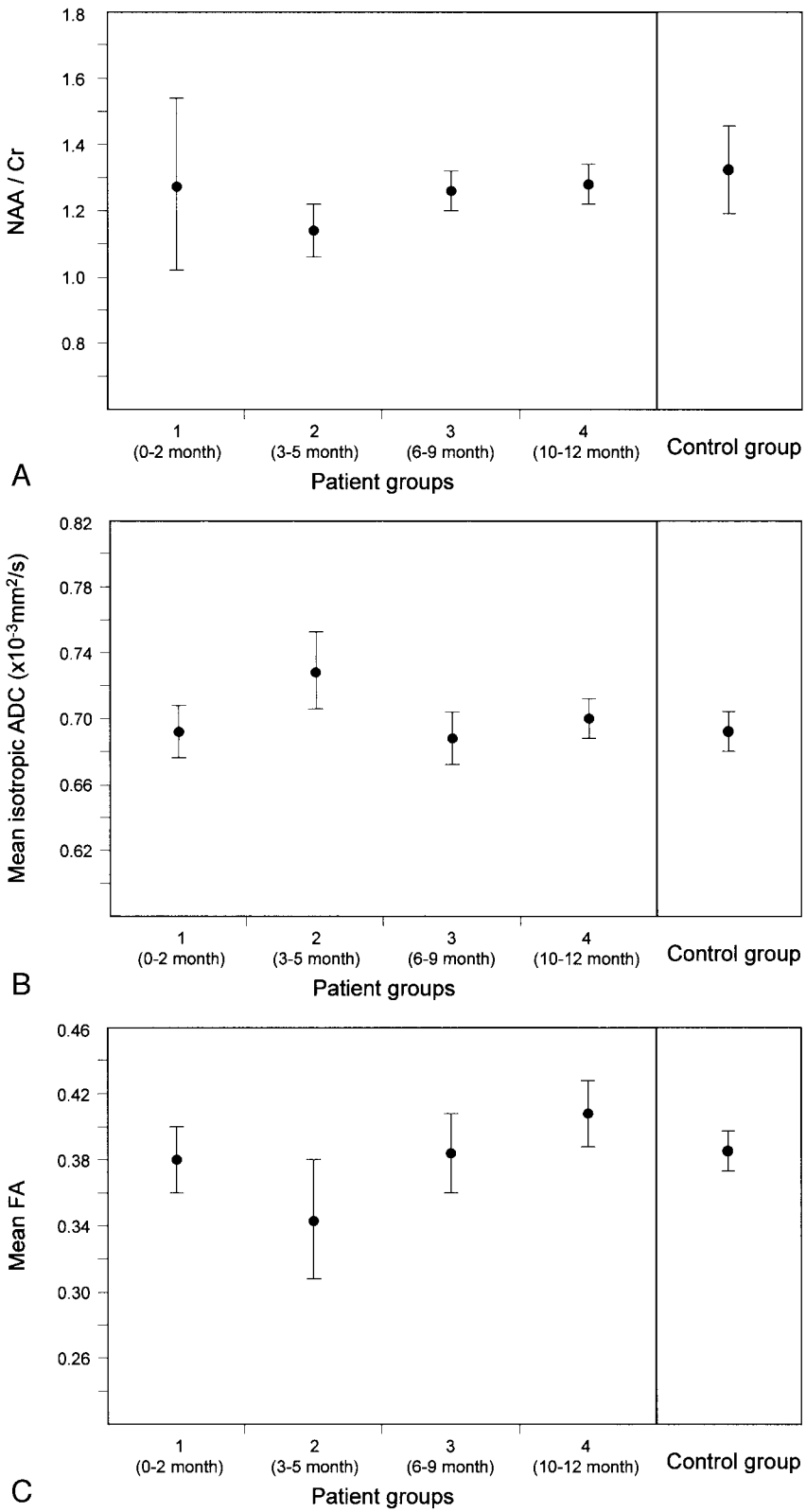

FIG 4. Temporal variations of the DT MR imaging and proton MR spectroscopy indices of the patient groups. Error bars represent the SDs of values.

A, NAA/Cr ratio. A reduction of average of NAA/Cr ratios of the patient group 2 is shown ($P = .04$).

B, Mean isotropic ADC value. An increase in average of mean isotropic ADC values of the patient group 2 is observed ($P = .0085$).

C, Mean FA value. A decrease in average of mean FA values of the patient group 2 is shown ($P = .004$).

isotropic ADC value), which the conventional MR images could not depict fully.

The increase in water content as a result of the vessel wall permeability alteration can contribute to increase in isotropic ADC value. As the edema subsides, the isotropic ADC value may return toward normal levels. Recovery of WM anisotropy has also been reported (26). In that report, it was considered that decreased anisotropy may result from both demyelination and vasogenic edema (26). In the present study, it was difficult to reveal whether there was demyelination in WM. The changes in the FA value

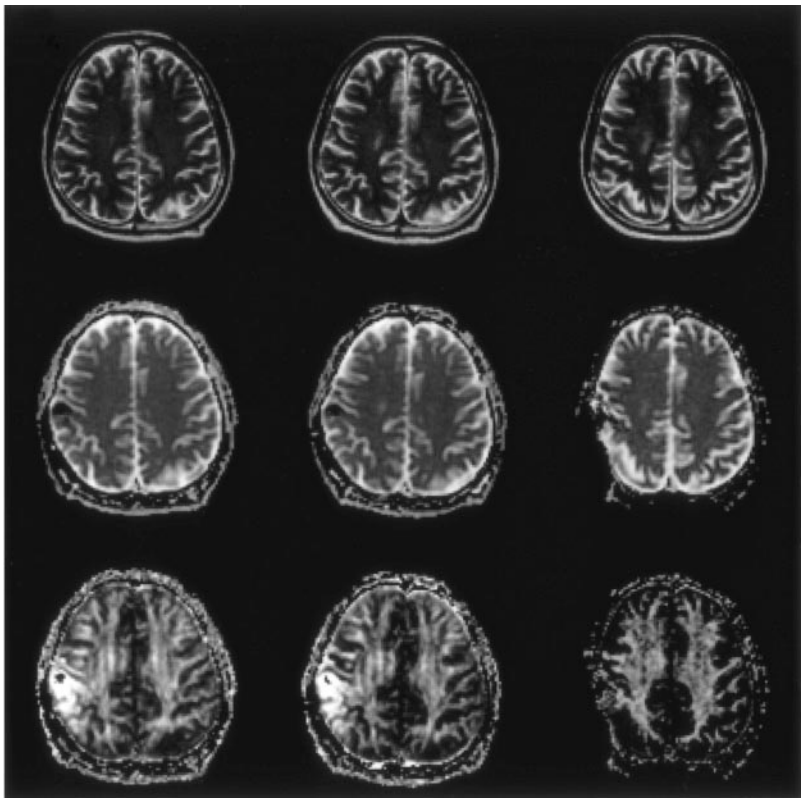

FIG 5. A 64-year-old man with total removal surgery for metastatic brain tumor, 30-Gy whole brain irradiation, and 15-Gy stereotactic radiosurgery (patient 5). The indices from only the left hemisphere were calculated because the right hemisphere had image distortion caused by the surgical procedure.

A, Axial T2-weighted images (TR/effective/TE/echo train length, 4000 ms/95 ms/18) at 4 (group 2; *left*), 8 (group 3, *middle*), and 12 months (group 4, *right*) following completion of radiation therapy show no abnormal intensity change in WM. At 12 months, slight increase in subarachnoid space of the right hemisphere is shown.

B, Isotropic ADC maps at 4 (*left*), 8 (*middle*), and 12 months (*right*) after completion of radiation therapy. Mean isotropic ADC values were 0.780, 0.707, and 0.720 ($\times 10^{-3}$ mm^2/s), respectively.

C, FA maps at 4 (*left*), 8 (*middle*), and 12 months (*right*) after completion of radiation therapy. Mean FA values were 0.32, 0.35, and 0.37, respectively. At 4 months after completion of radiation therapy, the mean FA value decreased and mean isotropic ADC value increased in comparison with the averages of mean FA value (0.38; SD = 0.02) and the mean isotropic ADC value (0.692; SD = 0.014) of the controls. The change of the indices appeared to resolve with time.

might be attributed to demyelination followed by remyelination as in the acute multiple sclerosis lesion (27). Only edematous change, however, can result in changes of both isotropic ADC value and FA value despite absence of demyelination or axonal injuries (26).

Proton MR spectroscopy can reveal radiation therapy–induced transient metabolic changes in the brain by using NAA as a probe. In a recent study, NAA/choline and NAA/Cr ratios decreased 4 months after starting radiation therapy (8). Similar transient NAA changes were observed in the present study. NAA decreases have been noticed in multiple sclerosis, strokes, primary and metastatic brain tumors, trauma, Alzheimer disease, and acquired immunodeficiency syndrome. Although the meaning of NAA change has not been fully analyzed, NAA is currently considered a neuron-specific metabolite and may be present in oligodendrocytes (28). A temporary dysfunction and loss of neuronal cells and/or myelinogenesis can contribute to the NAA change (28). It is also possible that regional volume changes may cause a decrease in the NAA concentration. This means that an increase in water content by edema, as may be seen in WM of the treated patients in the present study, can be attributed to the NAA change. Therefore, considering the possible histopathologic changes in WM of treated patients, the observed DT MR indices changes and the NAA change do not contradict each other.

Radiation therapy, chemotherapy, or both can contribute to the WM injury. Inhomogeneity of therapeutic modalities in the study group is one of limitations of our preliminary study. Radiation-induced changes have been categorized as acute, subacute, and late delayed effects. Acute radiation reactions occurring within weeks following radiation therapy are the result of transient vasodilation and increased capillary permeability leading to vasogenic edema (1). The acute effects are rare during conventional brain irradiation, except large fractionated radiation therapy or combined radiation therapy and chemotherapy (1, 3), and those kinds of therapies were not employed in the present study. Subacute reactions occur approximately between 2 and 6 months after radiation therapy (1, 14, 15). The period when the transient changes have been observed in the present study is within the period when the subacute reactions can develop. Lack of controls with chemotherapy and without radiation therapy is the limitation of our study to determine how chemotherapy contributes to the changes of indices. The relationship between irradiation dose and the frequency of the transient change was not clear, because of the small number of the subjects. To confirm these requires another study design with well-organized patient and control groups and strictly controlled follow-up MR imaging schedules.

Conclusion

In patients treated for brain tumors, mean isotropic ADC and FA values in segmented normal-appearing WM may be measured as quantitative indices for detecting the transient WM injuries revealed by proton MR spectroscopy. DT MR imaging seems to be a

potential method for objectively and quantitatively monitoring WM integrity after treatments, resulting in minimizing adverse effects to the normal brain tissues.

References

1. Schultheiss TE, Kun LE, Ang KK, Stephens LC. **Radiation response of the central nervous system.** *Int J Radiat Oncol Biol Phys* 1995;31:1093–1112
2. Ebner F, Ranner G, Slavc I, Urban C. **MR findings in methotrexate-induced CNS abnormalities.** *AJR Am J Roentgenol* 1989;153:1283–1288
3. Ball WS, Prenger EC, Ballard ET. **Neurotoxicity of radio/chemotherapy in children: pathologic and MR correlation.** *AJNR Am J Neuroradiol* 1992;13:761–776
4. Wilson DA, Nitschke R, Bowman ME, et al. **Transient white matter changes on MR images in children undergoing chemotherapy for acute lymphocytic leukemia: correlation with neuropsychologic deficiencies.** *Radiology* 1991;180:205–209
5. Stemmer SM, Stears JC, Burton BS, Jones RB. **White matter changes in patients with breast cancer treated with high-dose chemotherapy and autologous bone marrow support.** *AJNR Am J Neuroradiol* 1994;15:1267–1273
6. Basser PJ, Mattiello J, LeBihan D. **MR diffusion tensor spectroscopy and imaging.** *Biophys J* 1994;66:259–267
7. Khong PL, Kwong DL, Chan GC, et al. **Diffusion-tensor imaging for the detection and quantification of treatment-induced white matter injury in children with medulloblastoma: a pilot study.** *AJNR Am J Neuroradiol* 2003;24:734–740
8. Esteve F, Rubin C, Grand S, et al. **Transient metabolic changes observed with proton MR spectroscopy in normal human brain after radiation therapy.** *Int J Radiat Oncol Biol Phys* 1998;40: 279–286
9. Basser PJ, Pierpaoli C. **Microstructural and physiological features of tissues elucidated by quantitative-diffusion-tensor MRI.** *J Magn Reson B* 1996;111:209–219
10. Zhang Y, Brady M, Smith S. **Segmentation of brain MR images through a hidden Markov random field model and the expectation maximization algorithm.** *IEEE Trans Med Imaging* 2001;20:45–57
11. Smith S. **Fast robust automated brain extraction.** *Hum Brain Mapping* 2002;17:143–155
12. Jenkinson M, Bannister P, Brady J, Smith S. **Improved optimization for the robust and accurate linear registration and motion correction of brain images.** *Neuroimage* 2002;17:825–841
13. Provencher SW. **Estimation of metabolite concentrations from localized in vivo proton NMR spectra.** *Magn Reson Med* 1993;30:672–679
14. Armstrong C, Mollman J, Corn BW, et al. **Effects of radiation therapy on adult brain behavior: evidence for a rebound phenomenon in a phase 1 trial.** *Neurology* 1993;43:1961–1965
15. Lilja AM, Portin RI, Hamalainen PI, Salminen EK. **Short-term effects of radiotherapy on attention and memory performances in patients with brain tumors.** *Cancer* 2001;91:2361–2368
16. Szigety SK, Allen PS, Huyser-Wierenga D, Urtasun RC. **The effect of radiation on normal human CNS as detected by NMR spectroscopy.** *Int J Radiat Oncol Biol Phys* 1993;25:695–701
17. Vigliani MC, Sichez N, Poisson M, Delattre JY. **A prospective study of cognitive functions following conventional radiotherapy for supratentorial gliomas in young adults: 4-year results.** *Int J Radiat Oncol Biol Phys* 1996;35:527–533
18. Costello A, Shallice T, Gullan R, Beaney R. **The early effects of radiotherapy on intellectual and cognitive functioning in patients with frontal brain tumours: the use of a new neuropsychological methodology.** *J Neurooncol* 2004;67:351–359
19. Horsfield MA, Lai M, Webb SL, et al. **Apparent diffusion coefficients in benign and secondary progressive multiple sclerosis by nuclear magnetic resonance.** *Magn Reson Med* 1996;36:393–400
20. Guo AC, MacFall JR, Provenzale JM. **Multiple sclerosis: diffusion tensor MR imaging for evaluation of normal-appearing white matter.** *Radiology* 2002;222:729–736
21. Nusbaum AO, Tang CY, Buchsbaum MS, et al. **Regional and global changes in cerebral diffusion with normal aging.** *AJNR Am J Neuroradiol* 2001;22:136–142
22. Singer MB, Chong J, Lu D, et al. **Diffusion-weighted MRI in acute subcortical infarction.** *Stroke* 1998;29:133–136
23. Sorensen AG, Wu O, Copen WA, et al. **Human acute cerebral ischemia: detection of changes in water diffusion anisotropy by using MR imaging.** *Radiology* 1999;212:785–792
24. Brown MS, Stemmer SM, Simon JH, et al. **White matter disease induced by high-dose chemotherapy: longitudinal study with MR imaging and proton spectroscopy.** *AJNR Am J Neuroradiol* 1998;19:217–221
25. Moore AH, Olschowka JA, Williams JP, et al. **Radiation-induced edema is dependent on cyclooxygenase 2 activity in mouse brain.** *Radiat Res* 2004;161:153–160
26. Mukherjee P, McKinstry RC. **Reversible posterior leukoencephalopathy syndrome: evaluation with diffusion-tensor MR imaging.** *Radiology* 2001;219:756–765
27. Tievsky AL, Ptak T, Farkas J. **Investigation of apparent diffusion coefficient and diffusion tensor anisotropy in acute and chronic multiple sclerosis lesions.** *AJNR Am J Neuroradiol* 1999;20: 1491–1499
28. Bhakoo KK, Pearce D. **In vitro expression of N-acetyl aspartate by oligodendrocytes: implications for proton magnetic resonance spectroscopy signal in vivo.** *J Neurochem* 2000;74:254–262